

A Bayesian Nonparametric Approach to Reconstruction and Prediction of Random Dynamical Systems

Christos Merktas, Konstantinos Kaloudis and Spyridon J. Hatjispyros ¹

Department of Mathematics, University of the Aegean
Karlovassi, Samos, GR-832 00, Greece.

Abstract

We propose a Bayesian nonparametric mixture model for the reconstruction and prediction from observed time series data, of discretized stochastic dynamical systems, based on Markov Chain Monte Carlo methods (MCMC). Our results can be used by researchers in physical modeling interested in a fast and accurate estimation of low dimensional stochastic models when the size of the observed time series is small and the noise process (perhaps) is non-Gaussian. The inference procedure is demonstrated specifically in the case of polynomial maps of arbitrary degree and when a Geometric Stick Breaking mixture process prior over the space of densities, is applied to the additive errors.

Our method is parsimonious compared to Bayesian nonparametric techniques based on Dirichlet process mixtures, flexible and general. Simulations based on synthetic time series are presented.

Keywords: Bayesian nonparametric inference; Mixture of Dirichlet process; Geometric stick breaking weights; Random dynamical systems; Chaotic dynamical systems, Forecastable component analysis

1 Introduction

During the last three decades, nonlinear dynamical systems have been used to explain and model multiple time varying phenomena, exhibiting complex and irregular characteristics [35], finding applications in different fields of science such as physics, biology, computer science and economics. The erratic and unpredictable behavior of chaotic dynamics was early related to probabilistic and statistical methods of analysis [3, 4]. Nonlinearity alone though, is often not enough to properly describe the evolution of real physical phenomena, so the effect of noise has to be taken into account. In this respect, the constructed predictive model consists of two parts, the nonlinear-deterministic component and the random noise.

The source of the random noise influencing the procedure of interest is of great importance. If the origin of the noise is the uncertainty of the measurement process, then the available observations can be considered as the corruption of the true system states by measurement-observational noise and the dynamics of the process are not influenced. A widespread approach

¹Corresponding author. Tel.:+30 22730 82326
email address: schatz@aegean.gr

to confront this type of noise is the application of time delay embedding techniques and related methods, originating from the work of Takens [38]; see for example the review paper on the analysis of observed chaotic data by Abarbanel [1] and the book of Kantz [18] on the analysis of nonlinear time series and references therein.

Nevertheless, dynamical noise can drastically modify the underlying deterministic dynamics [14], as it represents the error in the assumed model, thus compensating for a small number of degrees of freedom. Dynamical systems subjected to the effects of dynamical noise are known as random dynamical systems [2, 46] and have many applications, mainly because dynamical noise is often present in real data. For the case of dynamical noise, the application of methods based on deterministic inference are not efficient, so many different methods have been proposed regarding the various aspects of the problem. In [31] a theorem was formulated to cope with the embedding problem for random dynamical systems, requiring multivariate observations. In [44] and [43] the issue of dynamical reconstruction was addressed for continuous time systems, by estimating drift and diffusion parameters of a Fokker-Plank equation under different types of perturbations. Due to the different impact of the noise types, the goal of discriminating between measurement and dynamical noise, as well as estimating the noise density, is highly significant [12, 42, 47].

Bayesian formulation [37] has been of great use in the general field of noise perturbed dynamical systems. It was initially demonstrated in this context by Davies [5], where MCMC methods were used for nonlinear noise reduction. In [27] and [28] MCMC methods were applied for the parameter estimation of state-space nonlinear models, extending maximum likelihood-based existing methods [25]. Later, in [45] a path integral representation was proposed for the likelihood function, in order to make inference in stochastic nonlinear dynamics, extended for nonstationary systems in [23]. In [24] and [32] Bayesian methods were suggested for reconstruction and prediction of nonlinear dynamical systems. Recently in [30], a Bayesian technique was proposed for the prognosis of the qualitative behavior of random dynamical systems under different forms of dynamical noise.

In this work, we will use a Bayesian approach to reconstruct and predict random dynamical systems. A common assumption in the literature is the normality of the noise process. Such an assumption cannot always be justified and can cause inferential problems when the noise process departs from normality, for example when it produces outlying errors. Then the estimated variance of the normal errors is artificially enlarged causing poor inference for the system parameters of interest. So for example we could have two sources of random perturbations. An environmental source caused by spatiotemporal inhomogeneities [47] producing weak and frequent perturbations, and, a high dimensional deterministic component interpreted in our model as stronger but less frequent perturbations in the form of outlying errors. Other cases include systems containing impulsive noise [29, 41], where the noise probability density function does not decay in the tails like Gaussian. Also, in situations where the system under consideration is coupled to multiple stochastic environments, the driving noise term may exhibit

non-Gaussian behavior, see for example references [17] and [16]. It is our intention therefore to model the dynamical noise using a highly flexible family of density functions, providing a Bayesian nonparametric formulation [6, 7]. We are confident that, contrary to the assumption of normality, our Bayesian modeling will be able to capture the right shape of the true underlying noise density hence leading to an improved and reliable statistical inference for the system even in cases where the size of the observed time series is small. Thus, if the number of noise sources is arbitrary, our approach is able to identify the true underlying model. This is because the different noise sources are represented by the active components of an infinite random mixture. Some recent applications of Bayesian nonparametric methods in nonlinear dynamical systems include Dirichlet process (DP) based reconstruction [11] and joint state-measurement noise density estimation with non-Gaussian and Gaussian observational and dynamical noise components respectively [15]. In this work we aim to:

1. Reconstruct dynamical equations and predict future values, by setting as a prior for the noise process a geometric stick breaking (GSB) mixture [7] which is effectively a random infinite mixture of probability kernels. Such a reconstruction involves the estimation of the unknown parameters of the deterministic part of the model, the initial condition responsible for the observed noisy time series and density estimation of the unknown and perhaps non-Gaussian error process.
2. Provide evidence, that modeling discrete time random dynamical systems via GSB mixtures, is efficient, faster and less complicated when compared to Bayesian nonparametric modeling via DP mixtures [11].
3. Show that sampling from the posterior joint distribution of the parameters, the initial condition and the future-unobserved-observation variables of the system, provides us with information for the long term behavior of the underlying process in the form of the quasi-invariant measure of the system.

The layout of the paper is as follows. In section 2, we are giving some preliminary notions in DP mixture priors, and we derive the two competing nonparametric inferential models. The first model is based on DP mixtures, and we develop its randomized-efficient version. It is based on the model that has been used for the reconstruction of random quadratic maps in [11]. It involves two infinite dimensional parameters in the form of random probability weights and locations. The second one, being our main contribution, is simpler and is based on GSB mixtures leading to a faster estimation algorithm as it involves only one infinite dimensional parameter in the form of locations. The GSB based Gibbs sampler is described in detail in section 3. In section 4 we specialize, for simplicity, to dynamical equations with polynomial nonlinearities to an arbitrary degree and we resort to simulation. We use simulated time series produced by a cubic map exhibiting complex dynamical behavior, that is dynamically perturbed by outlying errors of varying intensity. We compare the performance of the proposed GSB based Gibbs

sampler against its randomized DP based and plain parametric counterparts in the quality of reconstruction, out-of-sample forecasting and quasi-invariant measure estimation. To demonstrate the need for the nonparametric approach, we also compare the results with those obtained from a parametric Gibbs sampler assuming just Gaussian noise in the inferential procedure. In section 5 we conclude with a summary and future work. Finally, we offer five appendices as a supplementary material. In the supplementary file, appendix A, we provide embedded Gibbs sampling schemes for the various nonstandard densities arising in the implementation of the Gibbs samplers. In then supplementary file, appendix B, we obtain the invariant set of the deterministic part of the cubic map, which we have used for the generation of the synthetic time series for the illustration of our method. Also, in appendix C, we perform a comparison between the GSB sampler and a simple parametric MCMC, that assumes normal dynamical perturbations using noisy logistic time series. Finally, in appendix D we explain the dynamics exhibited by the cubic map used in our numerical experiments.

2 Preliminaries and derivation of the inferential models

A number of approaches have been proposed for system reconstruction. Maximum likelihood based methods treat the unknown parameters like fixed quantities, which maximize the joint conditional distribution of the observed values given the unknown parameters [10,19,25]. On the other hand Bayesian methods, assume that the parameters themselves are random variables; any prior knowledge can be incorporated together with the likelihood function in the form of the joint prior distribution of the parameters. Using Bayes theorem the posterior density, that is the conditional density of the system parameters given the observed time series, can be obtained. Here the most crucial step is to sample from the posterior density and thus to recover the marginal posterior density for each system parameter.

In related work [11], the assumption of normal errors is being relaxed; the additive independent and identically distributed (IID) dynamical noise is modeled with a family of density functions based on a Bayesian nonparametric model, the DP mixture model [22]. In their approach, they have modeled the random noise to have density

$$f_{\mathbb{P}}(z) = \int_{v>0} \mathcal{N}(z|0, v^{-1}) \mathbb{P}(dv), \quad (1)$$

where v is the precision of the zero mean normal distribution $\mathcal{N}(z|0, v^{-1})$ and $\mathbb{P} = \sum_{j \geq 1} w_j \delta_{\lambda_j} \sim \mathcal{DP}(c, P_0)$, is a discrete random probability measure defined over \mathbb{R}^+ , drawn from a DP [6] with concentration parameter $c > 0$ and base measure $P_0(dv) = \mathcal{G}(v|a, b)dv$, a gamma measure with shape a and rate b . The Dirac measures δ_{λ_j} are concentrated on the random precisions λ_j (the locations of \mathbb{P}) which are IID from P_0 . The random probability weights w_i are defined via a stick-breaking process [39, 40] so that $w_1 = z_1$ and for $j > 1$

$$w_j = z_j \prod_{s < j} (1 - z_s), \quad (2)$$

with the z_i variables IID from $\mathcal{B}e(1, c)$, a beta distribution with mean $(1 + c)^{-1}$.

Our intention is to reconstruct dynamical equations and jointly predict future values, by modeling additive noise components as geometric stick breaking mixture (GSBM) processes. We will show that GSBM modeling is as accurate as DPM modeling but less complicated and faster. Effectively, we will substitute the mixing measure \mathbb{P} in equation (1) by the random measure \mathbb{P}_G given by

$$\mathbb{P}_G = p \sum_{j=1}^{\infty} (1-p)^{j-1} \delta_{\lambda_j} \quad \text{with } p = (1+c)^{-1},$$

first introduced in Fuentes–Garcia et al. (2010). Mind that, although the random measure \mathbb{P}_G is closely related to $\mathbb{P} \sim \mathcal{DP}(c, P_0)$ (the measure \mathbb{P}_G is the expectation of \mathbb{P} given the random locations λ_j), \mathbb{P}_G is not of the Dirichlet type and is not a conjugate prior over the space of measures (see Ref. [26] and references therein).

2.1 The Model

We consider the following random dynamical model given by

$$X_i = T(\theta, X_{i-1}, Z_i) = g(\theta, X_{i-1}) + Z_i, \quad i \geq 1, \quad (3)$$

where $g : \Theta \times \mathbb{X} \rightarrow \mathbb{X}$, for some compact subset \mathbb{X} of \mathbb{R} , $(X_i)_{i \geq 0}$ and $(Z_i)_{i \geq 1}$ are real random variables over some probability space (Ω, \mathcal{F}, P) ; the set Θ denotes the parameter space and g is nonlinear, and for simplicity, continuous in X_{i-1} . We assume that the random variables Z_i are independent to each other, and independent of the states X_i . In addition we assume that the additive perturbations Z_i are identically distributed from a zero mean distribution with unknown density f defined over the real line, so that $T : \Theta \times \mathbb{X} \times \mathbb{R} \rightarrow \mathbb{R}$. We assume that there is no observational noise, so that we have at our disposal a time series $X^n = (x_1, \dots, x_n)$ generated by the Markovian processes defined in equation (3). The time series X^n depends solely on the initial distribution of X_0 , the vector of parameters θ , and the particular realization of the noise process.

We will model the errors in recurrence relation (3) as a random infinite mixture of zero mean normal kernels. As a mixing measure, initially we will use a general discrete random distribution $\mathbb{G} = \sum_{j \geq 1} \pi_j \delta_{\lambda_j}$ with random probability weights $\pi = (\pi_j)_{j \geq 1}$ and locations $\lambda = (\lambda_j)_{j \geq 1}$; then the conditional density of x given π and λ can be represented as

$$f_{\pi, \lambda}(x) = \int_{\mathbb{R}^+} \mathcal{N}(x|0, v^{-1}) \mathbb{G}(dv) = \sum_{j=1}^{\infty} \pi_j \mathcal{N}(x|0, \lambda_j^{-1}).$$

Conditionally on the variable x_0 , we have the transition kernels

$$f_{\pi, \lambda}(x_i | x_{i-1}, \theta) = \sum_{j=1}^{\infty} \pi_j \mathcal{N}(x_i | g(\theta, x_{i-1}), \lambda_j^{-1}), \quad 1 \leq i \leq n, \quad (4)$$

with associated data likelihood

$$f_{\pi,\lambda}(x_1, \dots, x_n | x_0, \theta) = \prod_{i=1}^n \sum_{j=1}^{\infty} \pi_j \mathcal{N}(x_i | g(\theta, x_{i-1}), \lambda_j^{-1}).$$

2.2 Dynamical Slice Sets

Due to the infinite mixture appearing in the product of the likelihood in the equation above, we are not able to construct Gibbs samplers of finite dimensions. To make the number of variables that we have to sample finite, we use slice sampling techniques for infinite mixtures. For each observation x_i , we introduce the pair (d_i, A_i) where d_i is the random variable that indicates the component of the infinite mixture the observation x_i came from, and A_i the associated x_i -slice set, which is a random almost surely finite set of indices. Marginally, we select each d_i with probability π_i that is $(d_i | \pi) \sim \sum_{j \geq 1} \pi_j \delta_j$, and the random variables d_i have an infinite state space. To have $(x_i | \lambda, A_i)$ coming from a finite mixture of normal kernels, a prerequisite that will enable us to create a Gibbs sampler with a finite number of updates, we let d_i conditionally on the event $(d_i \in A_i)$, to attain a discrete uniform distribution, that is

$$\begin{aligned} f_{\lambda}(x_i | A_i) &= \sum_{j=1}^{\infty} f_{\lambda}(d_i = j | A_i) f_{\lambda}(x_i | d_i = j) \\ &= \sum_{j \in A_i} |A_i|^{-1} \mathcal{N}(x_i | 0, \lambda_j^{-1}), \end{aligned}$$

where $|A_i|$ denotes the cardinality of the set A_i . Thus, given the precisions λ and the set A_i , the observation x_i comes from an equally weighted and almost surely finite mixture of normals.

We will consider two types of slice sets:

Non sequential slice sets. To each observation x_i , we assign the set $A_i = \{j \in \mathbb{N} : 0 < u_i < \pi_j\}$ [48] that depends on the weights π through the random variable u_i such that $f_{\pi}(d_i = j | u_i) \propto \pi_j \mathcal{U}(u_i | 0, \pi_j)$, where $\mathcal{U}(x | 0, \pi_j)$ denotes the uniform density over the interval $(0, \pi_j)$. Letting $\pi = w$, with w the stochastically ordered probability weights introduced in (2), for $1 \leq i \leq n$ we obtain a DP mixture based augmented random density

$$\begin{aligned} f_{w,\lambda}(x_i, u_i, d_i = j) &= w_j \mathcal{U}(u_i | 0, w_j) \\ &\quad \times \mathcal{N}(x_i | 0, \lambda_j^{-1}). \end{aligned} \tag{5}$$

Sequential slice sets. Letting $A_i = \{1, \dots, N_i\}$, with N_i being an almost surely finite discrete random variable of mass $f_N(\cdot | p)$, and letting $f(d_i = j | N_i) = N_i^{-1} \mathcal{I}(j \leq N_i)$ for $1 \leq i \leq n$ a discrete uniform distribution on the set A_i , we obtain a GSB mixture based augmented random density

$$\begin{aligned} f_{\lambda}(x_i, N_i = l, d_i = j) &= f_N(l | p) l^{-1} \\ &\quad \times \mathcal{I}(j \leq l) \mathcal{N}(x_i | 0, \lambda_j^{-1}). \end{aligned} \tag{6}$$

Marginalizing (6) with respect to (N_i, d_i) , it is that

$$f_\lambda(x_i) = \sum_{j=1}^{\infty} \pi_j \mathcal{N}(x_i | 0, \lambda_j^{-1}) \quad \text{with} \quad \pi_j = \sum_{l=j}^{\infty} l^{-1} f_N(l | p).$$

When N_i comes from the negative binomial distribution $f_N(l | p) = \mathcal{NB}(l | 2, p) = lp^2(1 - p)^{l-1} \mathcal{I}(l \geq 1)$, the weights π_j are geometric, that is

$$\pi_j = \sum_{l=j}^{\infty} l^{-1} f_N(l | p) = \sum_{l=j}^{\infty} l^{-1} lp^2(1 - p)^{l-1} = p(1 - p)^{j-1}. \quad (7)$$

The geometric weights can be thought of as a reparametrization of the expectation of the stick-breaking weights given in (2), in the sense that $\pi_j = \mathbb{E}(w_j)$ with $p = (1 + c)^{-1}$. Other distributions could be used as well but it is the $\mathcal{NB}(l | 2, p)$ that leads to a model with lesser complexity. It can be shown that the use of a $\mathcal{NB}(l | k, p)$ will give to the weights the form of a equally weighted mixture of Negative Binomial distributions that is $\pi_j = (k - 1)^{-1} \sum_{r=1}^{k-1} \mathcal{NB}(l | r, p)$.

2.3 The two dynamical reconstruction models

Now it becomes clear, that depending on the choice of the slice sets, we obtain two types of dynamical reconstruction models.

1. The DP mixture based model: From relations (4) and (5) it is that

$$\begin{aligned} f_{w,\lambda}(x_i, u_i, d_i = j | x_{i-1}, \theta) &= w_j \mathcal{U}(u_i | 0, w_j) \\ &\times \mathcal{N}(x_i | g(\theta, x_{i-1}), \lambda_j^{-1}). \end{aligned} \quad (8)$$

In a hierarchical fashion using the slice variables u_i and the stick-breaking representation we have that for $i = 1, \dots, n$ and $j \geq 1$:

$$\begin{aligned} (x_i | x_{i-1}, d_i = j, \theta, \lambda) &\stackrel{\text{IND}}{\sim} \mathcal{N}(g(\theta, x_{i-1}), \lambda_j^{-1}) \\ (u_i | d_i = j, w) &\stackrel{\text{IND}}{\sim} \mathcal{U}(0, w_j) \\ \text{P}(d_i = j | w) &= w_j \\ w_j = z_j \prod_{s < j} (1 - z_s), \quad z_j &\stackrel{\text{IID}}{\sim} \mathcal{Be}(1, c) \\ \lambda_j &\stackrel{\text{IID}}{\sim} P_0. \end{aligned}$$

2. The GSB mixture based model: From relations (4) and (6), and letting $f_N(\cdot | p) = \mathcal{NB}(\cdot | 2, p)$, we have

$$\begin{aligned} f_\lambda(x_i, N_i = l, d_i = j | x_{i-1}, \theta) &= \mathcal{NB}(l | 2, p) l^{-1} \mathcal{I}(j \leq l) \\ &\times \mathcal{N}(x_i | g(\theta, x_{i-1}), \lambda_j^{-1}). \end{aligned} \quad (9)$$

In a hierarchical fashion using the slice variables N_i we have that for $i = 1, \dots, n$ and $j \geq 1$:

$$\begin{aligned} (x_i | x_{i-1}, d_i = j, \theta, \lambda) &\stackrel{\text{IND}}{\sim} \mathcal{N}(g(\theta, x_{i-1}), \lambda_j^{-1}) \\ (d_i | N_i = l) &\stackrel{\text{IND}}{\sim} \mathcal{U}\{1, \dots, l\} \\ \pi_j &= \mathcal{NB}(j | 1, p), \quad N_i \stackrel{\text{IID}}{\sim} \mathcal{NB}(2, p) \\ \lambda_j &\stackrel{\text{IID}}{\sim} P_0, \end{aligned}$$

We have the following proposition:

Proposition 1. *The likelihoods $f_{w,\lambda}^{\mathcal{D}}$ and $f_{\lambda}^{\mathcal{G}}$ that include the T future unobserved values $(x_{n+1}, \dots, x_{n+T})$ of the observed series X^n , based on the DPM and GSBM models respectively, are given by:*

$$f_{w,\lambda}^{\mathcal{D}}(x_i, u_i, d_i, i = 1, \dots, n_T | \theta, x_0, c) \propto \prod_{\substack{1 \leq i \leq n_T \\ d_i: u_i < w_{d_i}}} \sqrt{\lambda_{d_i}} \exp \left\{ -\frac{\lambda_{d_i}}{2} h_{\theta}(x_i, x_{i-1}) \right\}, \quad (10)$$

and

$$f_{\lambda}^{\mathcal{G}}(x_i, N_i, d_i, i = 1, \dots, n_T | \theta, x_0, p) \propto \prod_{\substack{1 \leq i \leq n_T \\ d_i: d_i \leq N_i}} p^2 (1-p)^{N_i-1} \sqrt{\lambda_{d_i}} \exp \left\{ -\frac{\lambda_{d_i}}{2} h_{\theta}(x_i, x_{i-1}) \right\}, \quad (11)$$

where $h_{\theta}(x_i, x_{i-1}) = (x_i - g(\theta, x_{i-1}))^2$ and $n_T = n + T$.

Proof. The expressions for the two augmented data-likelihoods $f_{w,\lambda}^{\mathcal{D}}$ and $f_{\lambda}^{\mathcal{G}}$ are coming from equations (8) and (9) and their corresponding hierarchical representations. \square

It is now clear from the form of the likelihood that a Gibbs sampling scheme will have finite number of updates. The details of the GSB mixture based reconstruction model (from now on referred to as the GSBM model) is now described in Section 3. The implementation of the algorithm and further details involving the DP mixture based model, here generalized to a random concentration mass c (from now on referred to as the rDPR model) can be found in Hatjispyros et al. (2009).

3 Sampling algorithms

To choose the fittest between the rDPR and GSBM models, we adapt to a ‘‘synchronized’’ prior specification. More specifically, in this paper we use a fully stochastic version of the DPR algorithm, which involves imposing a $\mathcal{G}(\alpha, \beta)$ prior over the concentration parameter c as proposed by West in Ref [49]. (we remark that in [11], the concentration parameter c has been set to $c = 1$ through out the numerical experiments). Then, ‘‘synchronized’’ prior specifications involve a transformed gamma prior over the geometric probability p via $p = (1 + c)^{-1}$. So as a prior over p we set

$$f(p) = \mathcal{TG}(p | \alpha, \beta) = \frac{\beta^{\alpha} e^{\beta}}{\Gamma(\alpha)} p^{-(\alpha+1)} e^{-\beta/p} (1-p)^{\alpha-1}, \quad (12)$$

with $p \in (0, 1)$. Note that for generic applications of the GSBR model, a beta conjugate prior $f(p; \alpha, \beta) = \mathcal{B}e(p; \alpha, \beta)$ is preferable as it leads to an implementation of lesser complexity. We have noticed that both priors provide results that are nearly indistinguishable. As a base measure for both models, we use $P_0(d\lambda_j) = \mathcal{G}(\lambda_j|a, b)d\lambda_j$, $j \geq 1$ for fixed hyperparameters a and b .

Having completed the model, we are now ready to describe the Gibbs sampler and the full conditional densities for estimating the GSBR model. After initializing the variables d_i for $i = 1, \dots, n_T$ and the variables p, x_0 and θ , at each iteration, we will sample the variables:

$$(\lambda_j), 1 \leq j \leq N^*, \quad (d_i, N_i), 1 \leq i \leq n_T,$$

and

$$(\theta, x_0, p, z_{n_T+1}),$$

with $N^* = \max_{1 \leq i \leq n_T} N_i$.

1. We first sample the precisions λ_j for $j = 1, \dots, d^*$ and $d^* = \max_{1 \leq i \leq n_T} d_i$. We have that

$$f(\lambda_j | \dots) = \mathcal{G} \left(\lambda_j | a + \frac{1}{2} \sum_{i=1}^{n_T} \mathcal{I}(d_i = j), b + \frac{1}{2} \sum_{i=1}^{n_T} \mathcal{I}(d_i = j) h_\theta(x_i, x_{i-1}) \right),$$

where the expression $f(\lambda_j | \dots)$ denotes the density of λ_j conditional on the rest of the variables. If $N^* > d^*$ we sample the additional λ_j 's from the prior $\mathcal{G}(a, b)$.

2. We then sample the infinite mixture allocation variables d_i for $i = 1, \dots, n_T$. It is that

$$P(d_i = j | \dots) \propto \lambda_j^{1/2} \exp \left\{ -\frac{\lambda_j}{2} h_\theta(x_i, x_{i-1}) \right\} \mathcal{I}(j \leq N_i).$$

3. Next, to construct the sequential slice sets A_i for $1 \leq i \leq n_T$ we have to sample N_i from

$$P(N_i = l | d_i = j, \dots) \propto (1 - p)^l \mathcal{I}(l \geq j),$$

which is a truncated geometric distribution over the set $\{j, j + 1, \dots\}$.

4. The full conditional for x_0 , with a uniform prior over the set $\tilde{\mathbb{X}} \subseteq \mathbb{R}$ that represents our prior knowledge for the state space of the dynamical system in relation (3) will be

$$f(x_0 | \dots) \propto \mathcal{I}(x_0 \in \tilde{\mathbb{X}}) \exp \left\{ -\frac{\lambda_{d_1}}{2} h_\theta(x_1, x_0) \right\}. \quad (13)$$

5. The full conditional densities for the future unobserved observations, when $T \geq 2$ and for $j = 1, \dots, T - 1$, are given by

$$f(x_{n+j} | \dots) \propto \exp \left\{ -\frac{1}{2} [\lambda_{d_{n+j}} h_\theta(x_{n+j}, x_{n+j-1}) + \lambda_{d_{n+j+1}} h_\theta(x_{n+j+1}, x_{n+j})] \right\}. \quad (14)$$

For $j = T$ the full conditional is normal with mean $g(\theta, x_{n+T-1})$ and variance $\lambda_{d_{n+T}}^{-1}$, that is

$$f(x_{n+T} | \dots) = \mathcal{N}\left(x_{n+T} | g(\theta, x_{n+T-1}), \lambda_{d_{n+T}}^{-1}\right). \quad (15)$$

6. For the vector of parameters θ , and assuming a uniform prior over the subset $\tilde{\Theta}$ of the parameter space \mathbb{R}^k , the full conditional becomes

$$f(\theta | \dots) \propto \mathcal{I}(\theta \in \tilde{\Theta}) \exp\left\{-\frac{1}{2} \sum_{i=1}^{n_T} \lambda_{d_i} h_\theta(x_i, x_{i-1})\right\}. \quad (16)$$

7. Taking into consideration relation (12), the full conditional for the geometric probability p is

$$f(p | \dots) \propto p^{2n_T - \alpha - 1} (1 - p)^{L_{n_T}} e^{-\beta/p} \mathcal{I}(0 < p < 1), \quad (17)$$

where $L_{n_T} = \alpha + \sum_{i=1}^{n_T} N_i - n_T - 1$.

8. Having updated p , we construct the geometric weights π_j for $1 \leq j \leq N^*$ via equation (7). We are now ready to sample z_{n+1} from the noise predictive $f(z_{n+1} | x_1, \dots, x_n)$. At each iteration of the Gibbs sampler we have updated weights $(\pi_j)_{1 \leq j \leq N^*}$ and precisions $(\lambda_j)_{1 \leq j \leq N^*}$ and we sample independently $\rho \sim \mathcal{U}(0, 1)$. Then we take the λ_j with $1 \leq j \leq N^*$ satisfying

$$\sum_{i=0}^{j-1} \pi_i < \rho \leq \sum_{i=0}^j \pi_i, \quad \pi_0 = 0.$$

If $\rho > \sum_{i=0}^{N^*} \pi_i$, we sample λ_j from the prior $\mathcal{G}(a, b)$. In any case we sample z_{n+1} from the normal kernel $\mathcal{N}(0, \lambda_j^{-1})$.

Details on sampling efficiently via embedded Gibbs samplers, thus circumventing Metropolis-within-Gibbs implementations for the nonstandard densities arising in equations (13) through (17), are provided in the supplementary file appendix A.

4 Simulation Results

Quadratic polynomial maps, can exhibit for each parameter value at most one stable attractor. Multistability and coexistence of more than one strange attractors can be achieved under higher degree polynomial maps [20, 34]. We will generate observations from a cubic random map with a deterministic part given by

$$\tilde{g}(\vartheta, x) = 0.05 + \vartheta x - 0.99x^3. \quad (18)$$

When $\vartheta \in [\underline{\vartheta}, \bar{\vartheta}]$ with $\underline{\vartheta} = -0.04$ and $\bar{\vartheta} = 2.81$ the dynamics of \tilde{g} , starting from $x_0 = 1$, are bounded. The map becomes bistable in the regions under the extrema of (18) when $\vartheta \in \Theta_{\text{bi}} = [\underline{\vartheta}_{\text{bi}}, \bar{\vartheta}_{\text{bi}}]$ with $\underline{\vartheta}_{\text{bi}} = 1.27$ and $\bar{\vartheta}_{\text{bi}} = 2.54$. When $\vartheta > \bar{\vartheta}_{\text{bi}}$, the two coexisting chaotic attractors

collapse into one global attractor and the dynamics oscillate between the domains previously occupied by the isolated attractors. For more details concerning the dynamical behavior of the map given in relation (18) we refer to appendix D.

Noise processes: We illustrate the GSBP and rDPR models with simulated data sets, consisting of observations generated from the cubic random recurrence $x_i = \tilde{g}(\vartheta, x_{i-1}) + z_i$, for the specific parameter value $\vartheta^* = 2.55$ and initial condition $x_0 = 1$. The dynamical noise z_i was sampled from:

1. The equally weighted normal 4-mixture

$$f_1 = \sum_{r=0}^3 \frac{1}{4} \mathcal{N}(0, (5r+1)\sigma^2), \quad \sigma = 10^{-2}. \quad (19)$$

2. The normal 2-mixtures, which exhibit progressively heavier tails for $1 \leq l \leq 4$

$$f_{2,l} = \frac{5+l}{10} \mathcal{N}(0, \sigma^2) + \frac{5-l}{10} \mathcal{N}(0, (200\sigma)^2), \quad \sigma = 10^{-3}. \quad (20)$$

As a measure of the tail fatness of the density $z \sim f$, we use the mean absolute deviation from the mean normalized by the standard deviation, for a zero mean z it is that $TF_f = \mathbb{E}|z| / \sqrt{\mathbb{E}|z|^2}$. The closer TF_f is to 1, the thinner the tails are. It can be verified numerically that

$$TF_{f_1} > TF_{f_{2,1}} > \dots > TF_{f_{2,4}}.$$

We model the deterministic part $g(\theta, x)$ of the map in equation (3) with a polynomial in x of degree $m = 5$.

Our findings is that the GSBP models are more amenable to dynamical reconstruction purposes; they are as accurate as the DPR models, they give smaller execution times and are less complicated and thus easier to implement. In all the examples we also compare the results with the results obtained from a parametric reconstruction and prediction Gibbs sampler, that is assuming just Gaussian noise. We refer to this model as Param in the tables.

Prior specifications: Here we define the synchronized prior specifications of the GSBP and rDPR Gibbs samplers. We use the following general prior set up:

$$\begin{aligned} c &\sim \mathcal{G}(\alpha, \beta), & p &\sim \mathcal{TG}(\alpha, \beta), & \{\lambda_j &\sim \mathcal{G}(a, b) : j \geq 1\} \\ \theta &\sim \mathcal{U}((-M, M)^{k+1}), & x_0 &\sim \mathcal{U}(-M_0, M_0), \end{aligned}$$

where k is the degree of the modeling polynomial.

A. Noninformative reconstruction and prediction: In the absence of any prior knowledge, we propose a noninformative prior specification for simultaneous reconstruction and prediction, namely

$$\mathcal{PS}_{\text{NRP}} : \alpha = \beta \geq 10^{-1}, \quad a = b \geq 10^{-4}, \quad M \gg 1, \quad M_0 \gg 1.$$

B. Informative reconstruction and prediction: When a-priori we believe that the dynamical noise resembles a finite mixture of zero mean Gaussians with variances that are close to each other, we set:

$$\mathcal{PS}_{\text{IRP}} : \alpha > \beta \geq 10^{-1}, a > b \geq 10^{-4}, M \gg 1, M_0 \gg 1.$$

Such prior specifications induce a small average GSB probability p (and consequently a large average DP concentration mass c), forcing the Gibbs samplers to activate a large number of normal kernels. Thus generating a more detailed Gaussian mixture representation of the unknown dynamical noise.

Data sets and invariant sets: In Figure 1(a), we display the deterministic orbit of length 280 of the deterministic map $y_i = \tilde{g}(\vartheta^*, y_{i-1})$, with starting point at $y_0 = 1$. We have approximated the interval \mathbb{X} that is remaining invariant under the action of $\tilde{g}(\vartheta^*, \cdot)$ by $[-1.8881, 1, 8991]$ (see supplementary file, Appendix B), and the associated average characteristic Liapunov exponent by 0.4625. Realizations of the random recurrence $x_i = \tilde{g}(\vartheta^*, x_{i-1}) + z_i$, $x_0 = 1$ under different types of noise are given in Figures 1(b) and 1(c) respectively.

Our observations for reconstruction and out-of-sample prediction will be the data sets $X_{f_1}^{200}$ and $\{X_{f_{2,l}}^{200} : 1 \leq l \leq 4\}$. The latter data sets, have been generated in R under the random number generator seeds $RNG_{f_1} = 1$ and $RNG_{f_{2,l}:1 \leq l \leq 4} = \{10, 15, 13, 38\}$. Approximations of the deterministic and noisy invariant measures are given in Figures 1(d)-(f). The deterministic invariant measure $\mu_{\tilde{g},0}(dy)$ is approximated in Figure 1(d). The z -noisy measures $\mu_{\tilde{g},z}(dx)$ approximated in Figures 1(e) and 1(f), are quasi-invariant in the sense that for all measurable subsets B of \mathbb{R} it is that $\mu_{\tilde{g},z}(B) = \lim_{t \rightarrow \infty} \mathbb{P}(x_t \in B | \tau_{\mathbb{X}'} > t)$, where $\tau_{\mathbb{X}'}$ is a random time denoting the first time the system enters the trapping set \mathbb{X}' (see supplementary file, appendix B).

Complexity measures and prior specifications: The occurrence of an informative structure in the available data sets, may help the practitioner to decide between an informative and a noninformative prior set up. Approximate entropy (ApEn) [13, 36] can be used to assess the complexity of the available set $x_f^{(n)}$ of observations. Large ApEn values, indicate irregular and unpredictable time series data. Nevertheless, it is known that ApEn values are heavily dependent on sample size (lower than expected for small sample sizes). A recently developed complexity measure that is less dependent on the sample size, is the forecastable component analysis Ω (ForeCA) [8, 9], which is based on the entropy of the spectral density of the time series, and is normalized between zero and one. Large Ω values characterize more predictable time series.

In Figure 2 we display the Ω curves as functions of the sample size n , for the time series $X_{f_1}^n$ and $\{X_{f_{2,l}}^n : 1 \leq l \leq 4\}$. For the computation of the Ω curves we have used the weighted overlapping segment averaging (WOSA) method [9]. The data sets $\{X_{f_{2,l}}^n : 1 \leq l \leq 4\}$ have the more informative structure as for $n > 80$ and $1 \leq l \leq 4$ it is that

$$\Omega(X_{f_{2l}}^n) > \Omega(X_{f_1}^n).$$

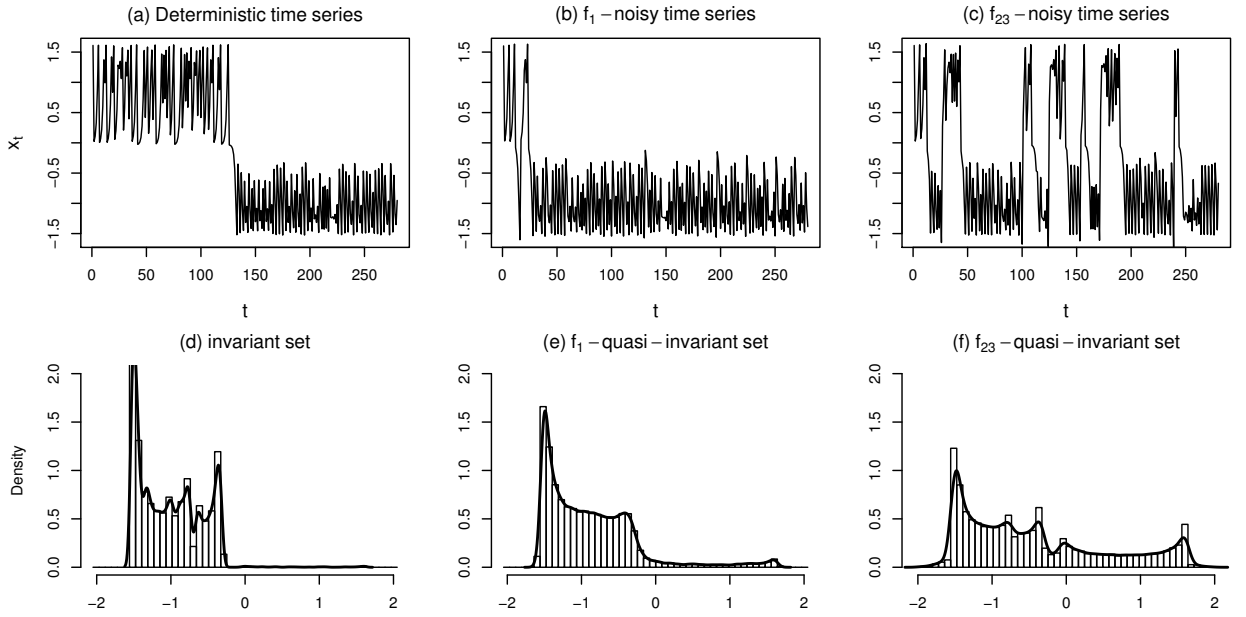


Figure 1: In figures 1(a)-(c) we display the deterministic orbit and f_1 and $f_{2,3}$ data-realizations with initial condition $x_0 = 1$. In figures 1(d)-(f) we display the deterministic invariant density approximation and the f_1 and $f_{2,3}$ quasi-invariant densities approximations respectively.

4.1 Informative reconstruction and prediction under the f_1 dynamic noise

We ran the Param, rDPR and GSBR Gibbs samplers for $T = 20$ in a synchronized mode, for 5×10^5 iterations and a burn-in period of 10,000, using data set $X_{f_1}^{200}$ under the informative prior specification $\mathcal{PS}_{\text{IRP}}$ with $\alpha = 3$, $\beta = 0.3$, $a = 1$, $b = 10^{-3}$ and $M = M_0 = 10$. We remark that under noninformative prior specifications of the form $\alpha = \beta \leq 0.3$, and $a = b \leq 10^{-3}$, the average number of active normals for both nonparametric samplers is lesser than four, leading to less accurate estimations. The following provide a summary and some brief comments.

Initial condition and dynamical noise density estimations: In Figure 3(a) we display kernel density estimations (KDE's) based on the predictive samples of the marginal posterior for the initial condition x_0 . The differences between the two predictives coming from the GSBR and rDPR samplers are indistinguishable. The three modes of the predictive density of x_0 are very close to the three real roots of the polynomial equation $\tilde{g}(\vartheta^*, x) - \tilde{g}(\vartheta^*, 1) = 0$ which are the preimages of $\tilde{g}(\vartheta^*, 1)$. Note that for $\vartheta \in (0.74, 2.97)$, it is that $\tilde{g}^{-1}(\vartheta, \tilde{g}(\vartheta, 1)) \in \{\rho, -1 - \rho, 1\}$ with $\rho = -(1 + \sqrt{4\vartheta/0.99 - 3})/2$. We refer to the three preimages of $\tilde{g}(\vartheta, 1)$ by $x_L = \rho$ (left), $x_M = -1 - \rho$ (middle) and $x_R = 1$ (right). In Figure 3(b), we give superimposed the noise predictives coming from the two models together with the true density of the noise component given in (19). We note how the synchronized execution produces almost identical dynamical

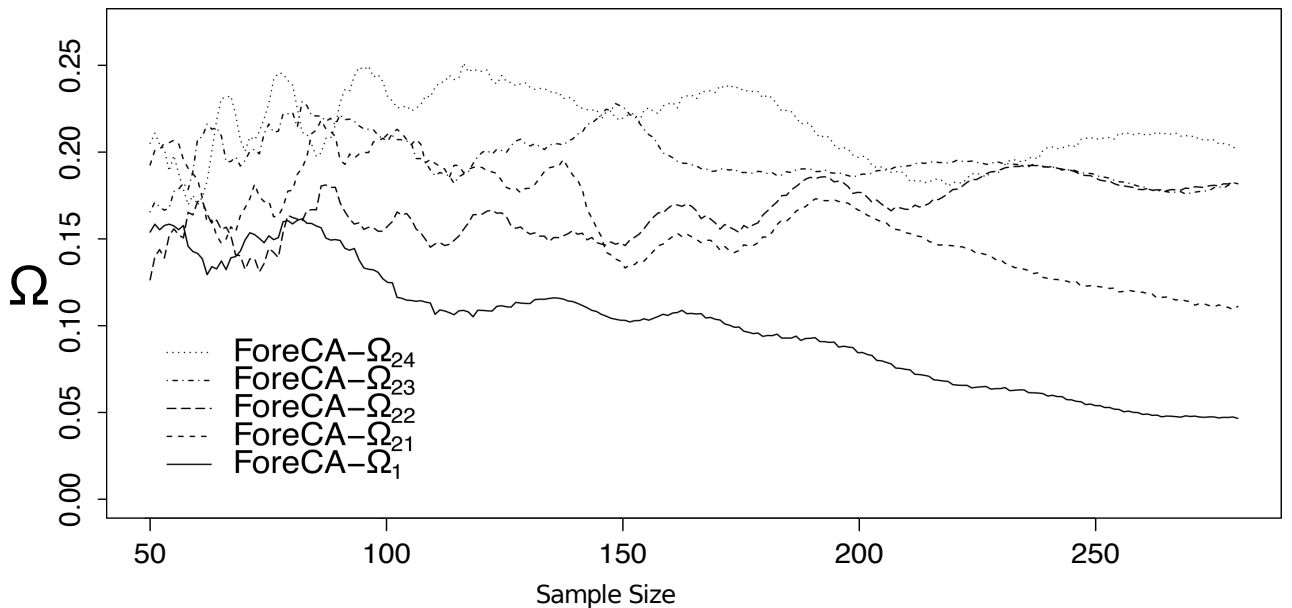


Figure 2: Here we display the Ω curves relating to the data sets $X_{f_1}^n$ and $\{X_{f_{2,l}}^n : 1 \leq l \leq 4\}$ for n between 50 and 280.

noise density estimations, which are very close to the true noise density f_1 (solid line in red).

In Figures 4(a)-(f), we plot the running ergodic averages for the θ_j variables of the first 80,000 iterations after burn-in. We observe that the θ_j chains have converged after the first 10,000 iterations, and that the chains are mixing well. In Table 1 we display the percentage absolute relative errors (PARE's) of the synchronized estimations. For each j , we have created $K = 47$ approximately independent samples of size $N = 10^4$, each sample separated by $s = 500$ observations

$$\{\theta_j^{(i_r)} : M_r + 1 \leq i_r \leq M_r + N\} \quad \text{with} \quad M_k = (k - 1)(N + s),$$

for $r = 1, \dots, K$. Then we created K realizations of the sampling mean (SM) estimator. Finally we took

$$\hat{\theta}_j = \frac{1}{K} \sum_{r=1}^K \frac{1}{N} \sum_{i=M_r+1}^{M_r+N} \theta_j^{(i)}, \quad 0 \leq j \leq 5.$$

We estimate x_0 by the maximum a-posteriori (MAP) of the x_0 predictive sample, by dividing the interval $[-2, 2]$ into 300 bins. We remark the accuracy and the closeness of the estimated θ values.

Out-of-sample posterior predictive marginals and the prediction barrier: In Figures 5(a)-(j) we display the KDEs of the marginal posterior predictive samples of the variables x_{201}, \dots, x_{205} and x_{216}, \dots, x_{220} coming from the GSBR (solid red line) and rDPR (dashed black line) superimposed. Together, we superimpose the f_1 quasi-invariant measure approximation (solid black line). We note how the synchronized execution produces almost identical posterior predictive marginals (PPM's). As the prediction horizon increases, the PPM densities are

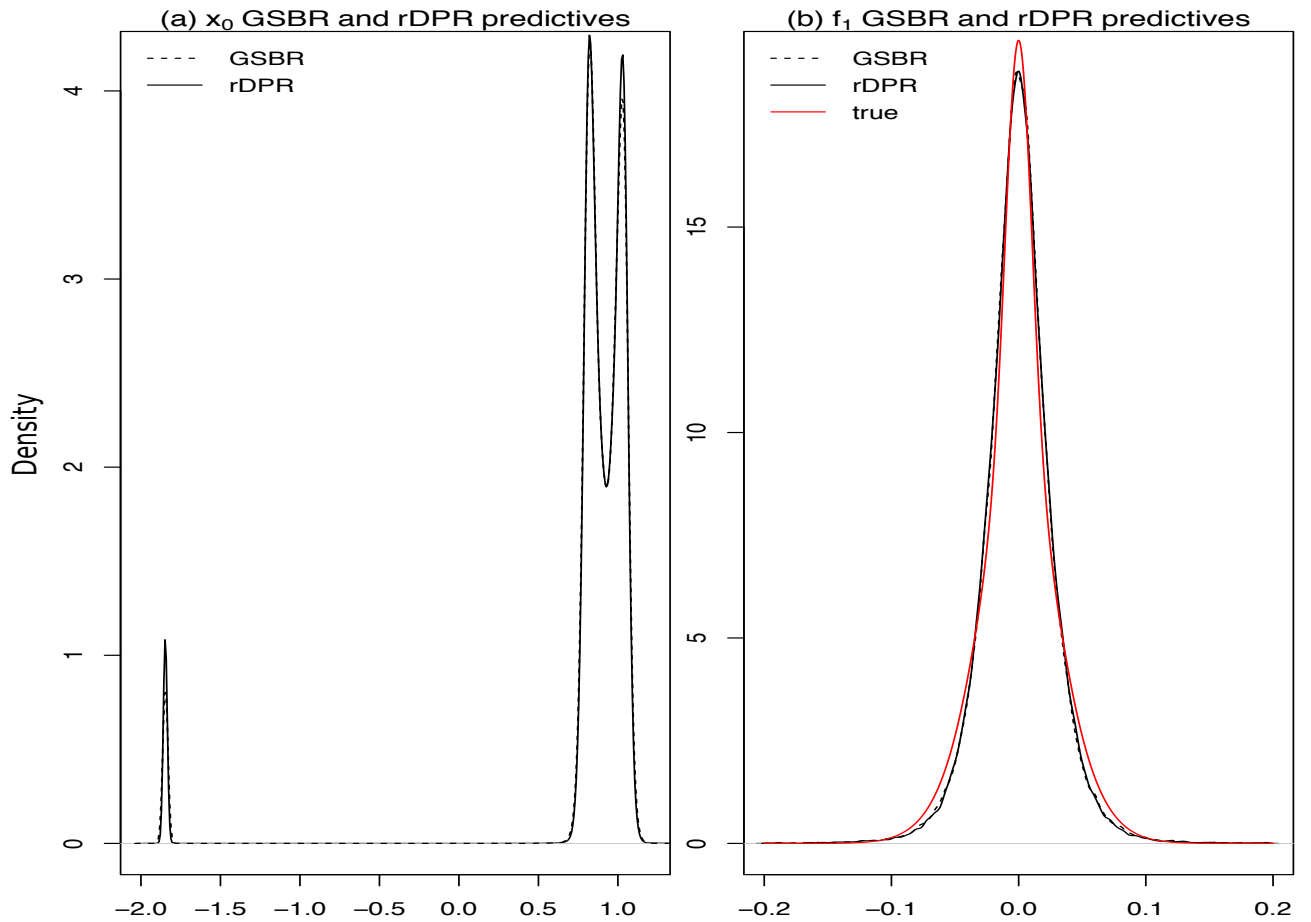


Figure 3: In Figure 3(a) we give superimposed the KDE's based on the posterior marginal predictive samples of the initial condition variable x_0 . In Figure 3(b) we superimpose the GSBR and the rDPR noise density estimations together with the true dynamical error density.

Model	θ_0	θ_1	θ_2	θ_3	θ_4	θ_5	x_0
Param.	1.98	0.37	0.03	0.58	0.00	0.04	$x_M : 3.87$
rDPR	0.81	0.29	0.01	0.09	0.04	0.14	$x_M : 0.80$
GSBR	0.19	0.27	0.05	0.04	0.02	0.18	$x_R : 0.60$
Estim.	x_{201}	x_{202}	x_{203}	x_{204}	x_{205}	GSBR-Av	Par-Av
SM	6.43	7.35	29.70	5.48	13.68	12.53	53.49
MAP	3.84	11.48	19.16	2.15	149.06	37.14	53.25

Table 1: (θ, x_0) reconstruction PAREs ($T = 0$) under the informative prior configuration.

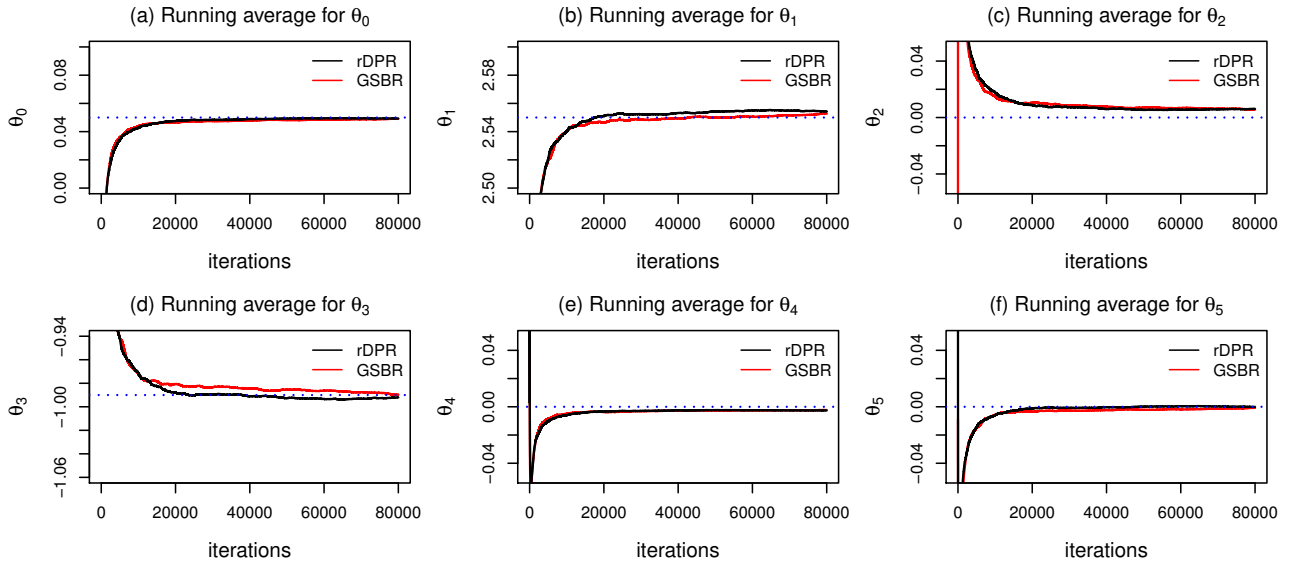


Figure 4: Chain ergodic averages for the θ_j variables based on the data set $x_{f_1}^{(100)}$, under prior specification \mathcal{PS}_{IR} , are superimposed in Figures 4(a)-(f).

Data set $X_{f_1}^{200}$			
Prior spec.	Algorithm	$T = 0$	$T = 20$
$\mathcal{PS}_{\text{IRP}}$	rDPR	5.44	11.76
$\mathcal{PS}_{\text{IRP}}$	GSBR	2.24	8.65

Table 2: Mean execution times in seconds per 10^3 iterations.

starting to resemble to the f_1 quasi-invariant density approximation, which naturally forms a prediction barrier. As such, any attempt to predict beyond this time horizon will replicate the quasi-invariant measure approximation. From this point on, we can make only probabilistic prediction arguments for the long term behavior of the system that involve the quasi-invariant measure i.e. $P(x_{n+i} \in A) = \mu_{\tilde{g},z}(A)$ for all $i \geq T$ and for all measurable subsets A of \mathbb{R} . In table 2, we give the mean computational time per 10^3 iterations relating to the synchronized execution of the rDPR and GSBR samplers under prior set up $\mathcal{PS}_{\text{IRP}}$ for a simple reconstruction ($T = 0$) and prediction ($T = 20$). In both cases, the GSBR sampler has the fastest execution times. In the last two rows of table 1 we give the PARE's of the first five GSBR out-of-sample predictions using the SM and MAP estimators. The last two columns exhibit the mean PARE's under a GSBR and a parametric prediction.

4.2 Noninformative reconstruction and prediction under the $f_{2,l}$ heavy tailed dynamic noise

Here we simultaneously reconstruct and predict using the noninformative prior set up. More specifically for $T = 20$ we set $\alpha = \beta = 0.3, a = b = 10^{-3}, M = M_0 = 10$; we iterated the GSBR

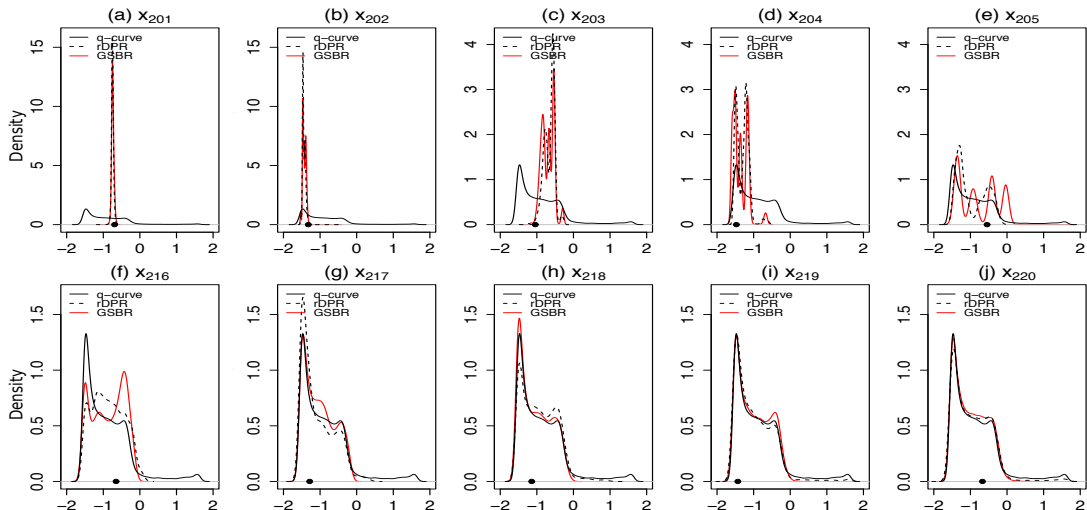


Figure 5: In Figures 5(a)-(j) we display superimposed the first five and the last five KDE's of the out-of-sample posterior marginal predictive based on data set $X_{f_1}^{200}$ under the informative specification $\mathcal{PS}_{\text{IRP}}$. Together we superimpose the KDE of the f_1 quasi invariant density (solid black line). In all Figures, the bullet point represents the corresponding true future value.

sampler 5×10^5 after a burn-in period of 10,000. In Figure 6 we display the KDE's based on the PPM samples of the out-of-sample variables $\{x_{201}, \dots, x_{205}\}$ and $\{x_{216}, \dots, x_{220}\}$ (solid lines in red) under data sets $X_{f_{2,l}}^{200} : 1 \leq l \leq 4$ (rows (a) to (d)). Together we superimpose the KDE of the associated quasi-invariant densities for $1 \leq l \leq 4$ (solid lines in black). In Tables 3 and 4 we display a PARE summary of (θ, x_0) estimations and out-of-sample prediction respectively, based on data sets $\{X_{f_{2,l}}^{200} : 1 \leq l \leq 4\}$. In table 3 we compare horizontally the PARE results coming from the GSB and the parametric sampler; we notice that in all cases, the accuracy of the GSB model is considerably higher than its parametric counterpart. In all cases, the parametric algorithm predicts a quintic polynomial deterministic part. Also, the GSB model precision improves as the noise model becomes more heavy tailed. In table 4 when we compare the average PARE results coming from the GSB and the parametric sampler (the last two columns) we notice that in all cases for both the SM and the MAP estimators, the prediction of the GSB model is considerably better. We also notice, that as we move to a more heavy tailed noise model, the GSB prediction gradually improves and the MAP-GSB estimator becomes more efficient. This is due to the multimodal nature of the PPM's generated by GSB.

5 Discussion

We have described a Bayesian nonparametric approach for dynamical reconstruction and prediction from observed time series data. The key insight is to use the GSB process, developed by Fuentes–García et al. (2010), as a prior (over the space of densities) on the noise component. The GSB model removes a level from the hierarchy of the rDPR model as it replaces the

Noise	Model	θ_0	θ_1	θ_2	θ_3	θ_4	θ_5	x_0
$f_{2,1}$	Param.	19.95	1.54	4.83	4.39	2.52	1.01	7.27
	GSBR	0.51	0.01	0.06	0.02	0.02	0.00	$x_R : 0.03$
$f_{2,2}$	Param.	2.89	0.94	4.07	2.37	2.07	0.76	7.49
	GSBR	0.54	0.05	0.06	0.12	0.03	0.03	$x_R : 0.03$
$f_{2,3}$	Param.	29.97	0.40	4.97	1.25	1.88	0.41	7.55
	GSBR	0.20	0.04	0.04	0.13	0.02	0.04	$x_R : 0.03$
$f_{2,4}$	Param.	15.57	1.07	1.33	3.71	0.43	1.03	6.40
	GSBR	0.10	0.01	0.05	0.03	0.01	0.00	$x_R : 0.03$

Table 3: Simultaneous reconstruction-prediction under the noninformative prior specification. The (θ, x_0) PARE's are based on the data sets $\{X_{f_{2,l}}^{200} : 1 \leq l \leq 4\}$ for $T = 20$.

Noise	Estim.	x_{201}	x_{202}	x_{203}	x_{204}	x_{205}	GSBR-Av	Par-Av
$f_{2,1}$	SM	12.50	0.86	12.57	44.04	82.11	30.42	58.72
	MAP	12.86	2.10	77.13	25.89	39.99	31.59	69.62
$f_{2,2}$	SM	0.52	0.70	8.07	167.16	15.17	38.32	65.08
	MAP	0.29	1.72	0.50	103.00	20.96	25.29	65.57
$f_{2,3}$	SM	0.72	7.99	0.01	9.74	49.94	13.68	233.53
	MAP	0.14	0.47	2.34	0.39	1.38	0.93	234.80
$f_{2,4}$	SM	0.24	1.01	2.95	3.79	40.25	9.65	60.69
	MAP	0.07	0.86	4.78	0.13	21.00	5.37	109.23

Table 4: Simultaneous reconstruction-prediction under the noninformative prior specification. The out-of-sample PARE's are based on data sets $\{X_{f_{2,l}}^{200} : 1 \leq l \leq 4\}$ for $T = 20$. The GSBR-Av and Par-Av columns are the PARE means of the first five out-of-sample estimations using the GSBR and the parametric Gibbs samplers respectively.

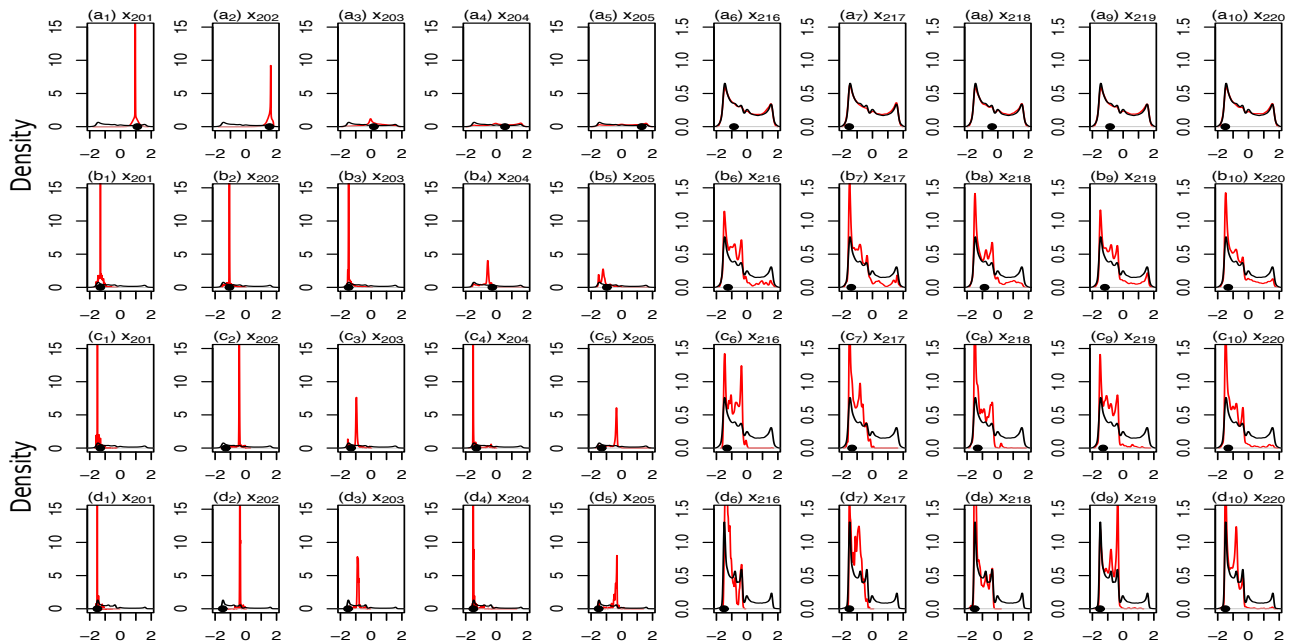


Figure 6: In Figure 6 we display the GSB KDE's of the PPM sample of the out-of-sample variables $\{x_{201}, \dots, x_{205}\}$ and $\{x_{216}, \dots, x_{220}\}$ (solid lines in red) based on samples $X_{f_{2,l}}^{200} : 1 \leq l \leq 4$ (rows (a) to (d)) under the noninformative prior specification. Together we superimpose the KDE of the $f_{2,l}$ quasi-invariant densities for $1 \leq l \leq 4$ (solid lines in black).

weights of the stick breaking representation of the DP with their expected values, leading to a simpler model with only one infinite dimensional parameter, the locations of the atoms (λ_j) of the random measure. GSB mixture dynamical modeling is as accurate as DP based modeling but it gives smaller execution times, and is easier to implement.

We have also shown that in a joint prediction of future values of a low dimensional noisy chaotic time series, the quasi-invariant set appears as a “prediction barrier”. Also, our numerical experiments indicate that when the sample size of the time series is small, the forecastable component analysis Ω measure can group the available sets of observations in terms of their complexity. A larger Ω index suggests a less informative prior set up. We note, that when there is strong evidence that the dynamical error has a Gaussian distribution, and the length of the observed time series is large, the application of nonparametric models is superfluous. Nevertheless, when the size of the observed time series is very small and the dynamical errors are Gaussian, the accuracy of the simple MCMC (Param.) depends heavily on the particular realization of the noise process. Then the application of the GSB based algorithm will be in principle more accurate. Infinite mixtures of zero mean Gaussians, can mimic the effect of any heavy tailed symmetric noise processes, of finite or infinite kurtosis to an arbitrary level of accuracy. Hence, natural directions for our future research interests include:

1. Estimation and prediction of dynamical systems perturbed by impulsive dynamic noise: We believe that in this case the prior for the noise component should have the

mixed type representation

$$F(dz) = q \sum_{j=1}^{\infty} \pi_j \mathcal{N}(z|0, \lambda_j^{-1}) dz + (1 - q) \delta_0(dz),$$

with $q \sim \mathcal{B}e(h_1, h_2)$, which is a random mixture of a Dirac measure concentrated at zero and a GSB mixture of zero mean normal kernels.

2. Estimation and prediction of dynamical systems under strong and persistent dynamic perturbations: It is possible that the coexistence of a large number of active components (informative prior set up) and strong and persistent dynamic noise when $T > 0$, will affect the mixing properties of the θ component of the Gibbs sampler; thus producing biased estimations of the θ_i 's. A possible solution to this problem could be the introduction of a (θ, ϵ) -constrained Gibbs sampler together with an adaptive Gibbs scheme for the out-of-sample variables. More specifically, when $\max_{0 \leq j \leq k} |(\hat{\theta}_j^* - \hat{\theta}_j)/\hat{\theta}_j^*| > \epsilon$, where $\hat{\theta}^*$ is the reconstruction ($T = 0$) estimation, and ϵ a small predefined constant, we propose the restriction of the θ prior specification to:

$$\theta \sim \mathcal{U} \left(\prod_{j=0}^k (\hat{\theta}_j^* - \epsilon_j, \hat{\theta}_j^* + \epsilon_j) \right), \quad \max_j \epsilon_j < \epsilon.$$

When the mixing properties of the out-of-sample variables components of the Gibbs sampler are affected, very long chains are needed to achieve convergence. In that case, we could resort to more sophisticated Monte Carlo schemes to improve the sampling efficiency, such as hybrid Monte Carlo [33], or adaptive random scan sampling [21], in order to improve the sampling efficiency.

3. When the data available are contaminated with dynamical and observational noise: We can extend the GSBR model to a q -lagged state space model, more precisely

$$\begin{aligned} X_i &= g(\theta, X_{i-1}, \dots, X_{i-q}) + Z_i, \quad i \geq q \\ Y_i &= h(\phi, X_i) + W_i, \end{aligned}$$

for some function h . Here we assume that noisy measurements of the output occur at all times, making the X^n sequence unobservable. The set of observations in this case is the Y^n time series, which can be modeled via a GSB random measure \mathbb{P}_Y . Then the latent X^n series can be modeled with a second independent GSB random measure \mathbb{P}_X , such that the random variables $[X_i | X_{i-1}, \dots, X_{i-p}, \theta, \mathbb{P}_X]$ and $[Y_i | X_i, \phi, \mathbb{P}_Y]$ are independent. In this case we have to estimate the initial condition $(X_0, \dots, X_{q-1}, Y_0)$, the parameter (θ, ϕ) , the density of the noise component (Z_i, W_i) as well as the hidden orbit $\{X_i : i = q, \dots, n\}$.

Acknowledgments

The second author is funded by the ‘‘Ypatia’’ scholarship program of the University of the Aegean.

Supplementary material

In this section we provide the Appendices A,B,C and D referenced on the text.

Appendix A: Sampling from nonstandard full conditionals

Here we adapt our calculations for the specific case where the deterministic part is a polynomial of degree m , namely $g(\theta, x) = \sum_{k=0}^m \theta_k x^k$.

1. Sampling the θ -coefficients: From equation (16) in the main text and for $j = 1, \dots, m$ it is that

$$f(\theta_j | \dots) \propto \mathcal{I}(\theta \in \tilde{\Theta}_j) \exp \left\{ -\frac{1}{2} \sum_{i=1}^n \lambda_{d_i} h_\theta(x_i, x_{i-1}) \right\}, \quad (21)$$

where $\tilde{\Theta}_j$ is the j -th projection interval of the set $\tilde{\Theta}$. Letting $\xi_{ji} := x_i - \sum_{k \neq j}^m \theta_k x_{i-1}^k$, we obtain the full conditional for θ_j , which is a normal truncated over the set $\tilde{\Theta}_j$ given by

$$f(\theta_j | \dots) \propto \mathcal{I}(\theta \in \tilde{\Theta}_j) \mathcal{N}(\theta_j | \mu_j, \tau_j^{-1}) \quad (22)$$

with

$$\mu_j := \tau_j^{-1} \sum_{i=1}^n \lambda_{d_i} \xi_{ji} x_{i-1}^j, \quad \tau_j := \sum_{i=1}^n \lambda_{d_i} x_{i-1}^{2j}.$$

To sample from this density, a-priori we set $\theta_j \in \tilde{\Theta}_j := (\theta_j^-, \theta_j^+)$ and we augment the θ_j full conditionals by the auxiliary variables θ'_j [?] such that jointly

$$f(\theta_j, \theta'_j | \dots) \propto \mathcal{U}(\theta_j | \theta_j^-, \theta_j^+) \mathcal{I}(\theta'_j > (\theta_j - \mu_j)^2) e^{-\tau_j \theta'_j / 2}. \quad (23)$$

Then we have the following Lemma:

Lemma A.1 *The augmentation of the full conditionals of θ_j for $j = 1, \dots, m$ with the positive random variables θ'_j such that they jointly satisfy (23), leads to the following embedded Gibbs sampling scheme:*

$$\begin{aligned} f(\theta'_j | \theta_j, \dots) &\propto \mathcal{E}(\theta'_j | \tau_j / 2) \mathcal{I}(\theta'_j > (\theta_j - \mu_j)^2) \\ f(\theta_j | \theta'_j, \dots) &= \mathcal{U}(\theta_j | \alpha_j, \beta_j), \quad \alpha_j := \max\{\theta_j^-, \mu_j - \theta_j'^{1/2}\}, \quad \beta_j := \min\{\theta_j^+, \mu_j + \theta_j'^{1/2}\}. \end{aligned}$$

where $\mathcal{E}(\theta'_j | \tau_j / 2)$ denotes the exponential density with rate $\tau_j / 2$.

Proof: These are the full conditionals of the bivariate density given in equation (23). \square

Sampling the initial condition: Similarly, to sample from the full conditional of x_0 in relation (13) given in the main text, we introduce the variable x'_0 such that

$$f(x_0, x'_0 | \dots) \propto \mathcal{I}(x_0 \in \tilde{X}) \mathcal{I}(x'_0 > h_\theta(x_1, x_0)) e^{-\lambda_{d_1} x'_0 / 2}.$$

Clearly, the full conditional of x'_0 is an exponential of rate $\lambda_{d_1}/2$, truncated over the interval $(h_\theta(x_1, x_0), \infty)$. The new full conditional for x_0 is a mixture of at most m uniforms given by

$$f(x_0|x'_0, \dots) \propto \mathcal{I}(x_0 \in \tilde{X}) \mathcal{I}(x_0 \in \mathcal{R}_g), \quad \mathcal{R}_g := \{x : \underline{x}_0 < g(\theta, x) < \bar{x}_0\}, \quad (24)$$

where $\underline{x}_0 := x_1 - x_0^{1/2}$ and $\bar{x}_0 := x_1 + x_0^{1/2}$. The set \mathcal{R}_g can be represented as the union of intervals, with boundaries defined by the real roots of the two polynomial equations

$$\underline{q}(x_0) := g(\theta, x_0) - \underline{x}_0 = 0, \quad \bar{q}(x_0) := g(\theta, x_0) - \bar{x}_0 = 0. \quad (25)$$

More specifically, we are going to show that there is $r \leq m$ such that

$$\mathcal{R}_g = \bigcup_{i=1}^r (\rho_{2i-1}, \rho_{2i}), \quad (26)$$

with $\{\rho_1, \dots, \rho_{2r}\}$ the ordered set of the real roots of the two polynomial equations in (25). In the sequel we make use of the following notation

$$\begin{aligned} \{\bar{q} < 0\} &:= \{x_0 \in \mathbb{R} : \bar{q}(x_0) < 0\}, \\ \{\underline{q} > 0\} &:= \{x_0 \in \mathbb{R} : \underline{q}(x_0) > 0\}. \end{aligned}$$

First we will consider the two even degree cases. When the leading coefficient is positive, the equation $\bar{q} = 0$ has at least two real roots. If there are more than two real roots, their number will be a multiple of two. On the other hand, when $\underline{q} = 0$ has real solutions their number will be even. Then for $s' \geq 1$ and $t' \geq 0$ it is that

$$\{\bar{q} < 0\} = (\bar{\rho}_1, \bar{\rho}_2) \cup \dots \cup (\bar{\rho}_{2s'-1}, \bar{\rho}_{2s'}) \quad (27)$$

$$\{\underline{q} > 0\} = (-\infty, \underline{\rho}_1) \cup \dots \cup (\underline{\rho}_{2t'}, \infty). \quad (28)$$

When $t' \geq 1$ it is that $\bar{\rho}_1 < \underline{\rho}_1 < \underline{\rho}_{2t'} < \bar{\rho}_{2s'}$. Therefore $r = 2(s' + t')$ and the intersection of the two sets $\{\bar{q} < 0\}$ and $\{\underline{q} > 0\}$ is of the form (26). When the leading coefficient is negative the result is similar with the right hand sides of equations (27) and (28) interchanged.

When the degree is odd and the leading coefficient is positive, both equations $\bar{q} = 0$ and $\underline{q} = 0$ have at least one real solution $\bar{\rho}_1$ and $\underline{\rho}_1$ respectively, with $\underline{\rho}_1 < \bar{\rho}_1$. If some of the two equations have more than one real solution, the number of the additional roots will be a multiple of two. So for $s' \geq 0$ and $t' \geq 0$ it is that

$$\{\bar{q} < 0\} = (-\infty, \bar{\rho}_1) \cup (\bar{\rho}_2, \bar{\rho}_3) \cup \dots \cup (\bar{\rho}_{2s'}, \bar{\rho}_{2s'+1}) \quad (29)$$

$$\{\underline{q} > 0\} = (\underline{\rho}_1, \underline{\rho}_2) \cup \dots \cup (\underline{\rho}_{2t'-1}, \underline{\rho}_{2t'}) \cup (\underline{\rho}_{2t'+1}, \infty). \quad (30)$$

For $s' \geq 1$ and $t' \geq 1$ we have $\underline{\rho}_1 < \bar{\rho}_1 < \underline{\rho}_{2t'+1} < \bar{\rho}_{2s'+1}$, and $r = 2(s' + t' + 1)$ which shows that the intersection of the two sets $\{\bar{q} < 0\}$ and $\{\underline{q} > 0\}$ is of the form (26). When the leading

coefficient is negative the result is similar with the right hand sides of the equations (29) and (30) interchanged.

So we have proved the following lemma:

Lemma A.2 *The augmentation of the full conditional of x_0 with the positive random variable x'_0 leads to the following embedded Gibbs sampling scheme:*

$$\begin{aligned} f(x'_0|x_0, \dots) &\propto \mathcal{E}(x'_0|\lambda_{d_1}/2) \mathcal{I}(x'_0 > h_\theta(x_1, x_0)) \\ f(x_0|x'_0, \dots) &\propto \mathcal{I}(x_0 \in \tilde{X}) \mathcal{I}(x_0 \in \bigcup_{i=1}^r (\rho_{2i-1}, \rho_{2i})), \end{aligned}$$

for some $r \leq m$, with $\{\rho_1, \dots, \rho_{2r}\}$ being the ordered set of the real roots of the two polynomial equations in (25).

2. Sampling the first $T - 1$ future observations: The full conditionals x_{n+j} for $1 \leq j \leq T - 1$ in relation (14) given in the main text are nonstandard densities. We augment the conditional of x_{n+j} with the pair of variables (x'_{n+j}, x''_{n+j}) such that jointly

$$\begin{aligned} f(x_{n+j}, x'_{n+j}, x''_{n+j} | \dots) &\propto e^{-\frac{1}{2}\lambda_{d_{n+j}}x'_{n+j}} \mathcal{I}(x'_{n+j} > h_\theta(x_{n+j}, x_{n+j-1})) \\ &\times e^{-\frac{1}{2}\lambda_{d_{n+j+1}}x''_{n+j}} \mathcal{I}(x''_{n+j} > h_\theta(x_{n+j+1}, x_{n+j})). \end{aligned}$$

The full conditionals of x'_{n+j} and x''_{n+j} are truncated exponentials with rates $\lambda_{d_{n+j}}/2$ and $\lambda_{d_{n+j+1}}/2$ over the intervals $(h_\theta(x_{n+j}, x_{n+j-1}), \infty)$ and $(h_\theta(x_{n+j+1}, x_{n+j}), \infty)$ respectively.

The full conditional of x_{n+j} is of the form (24) with the set \tilde{X} replaced by the set (x_{n+j}^-, x_{n+j}^+) with $x_{n+j}^\pm := g(\theta, x_{n+j-1}) \pm x_{n+j}^{1/2}$, and the set \mathcal{R}_g replaced by the set $\{x : \underline{x}_{n+j} < g(\theta, x) < \bar{x}_{n+j}\}$ with $\underline{x}_{n+j} := x_{n+j+1} - x_{n+j}^{1/2}$ and $\bar{x}_{n+j} := x_{n+j+1} + x_{n+j}^{1/2}$.

3. Sampling the geometric probability p : To sample from the density in relation (17) in the main text we include the pair of positive auxiliary random variables p_1 and p_2 such that

$$f(p, p_1, p_2 | \dots) \propto p^{2n_T - \alpha - 1} \mathcal{I}(p_1 < (1 - p)^{L_{n_T}}) \mathcal{I}(p_2 < e^{-\beta/p}),$$

with $p \in (0, 1)$. The full conditionals for p_1 and p_2 are uniforms

$$f(p_1 | \dots) = \mathcal{U}(p_1 | 0, (1 - p)^{L_{n_T}}), \quad f(p_2 | \dots) = \mathcal{U}(p_2 | 0, e^{-\beta/p}).$$

The new full conditional for p becomes

$$f(p | p_1, p_2, \dots) \propto p^{2n_T - \alpha - 1} \begin{cases} \mathcal{I}\left(-\frac{\beta}{\log p_2} < p < 1 - p_1^{1/L_{n_T}}\right) & L_{n_T} \geq 0 \\ \mathcal{I}\left(\max\left\{-\frac{\beta}{\log p_2}, 1 - p_1^{1/L_{n_T}}\right\} < p < 1\right) & L_{n_T} < 0. \end{cases}$$

We can sample from this density using the inverse cumulative distribution function technique.

We note that for a standalone application of the GSBR sampler, a beta prior distribution for p is more preferable as it leads to an implementation of a lesser complexity (in our paper

we have chosen to assign a transformed gamma prior merely for comparison purposes). Letting $f(p; \alpha, \beta) = \mathcal{B}e(p; \alpha, \beta) \propto p^{\alpha-1}(1-p)^{\beta-1}$ and using the GSB likelihood given in main text equation (11) we obtain

$$f(p | \dots) \propto p^{\alpha+2n_T-1}(1-p)^{\beta+\sum_{i=1}^{n_T} N_i-1},$$

which is a beta density with shapes $\alpha + 2n_T$ and $\beta + \sum_{i=1}^{n_T} N_i$.

Appendix B: The invariant set of the polynomial map

$$x' = \tilde{g}(\vartheta^*, x)$$

For $\vartheta = \vartheta^* = 2.55$ we let

$$\tilde{g}(x) \equiv \tilde{g}(\vartheta^*, x) = 0.05 + 2.55x - 0.99x^3,$$

and we define $\tilde{g}^{(n)}$ to be the n -fold composition of \tilde{g} with itself. We let $\mathcal{R}^{(2)}$ to be the set of real roots of the polynomial equation $\tilde{g}^{(2)}(x) = x$, with $\underline{x} = \min \mathcal{R}^{(2)}$, $\bar{x} = \max \mathcal{R}^{(2)}$ and $\mathbb{X} = [\underline{x}, \bar{x}]$. We denote the complement of \mathbb{X} by $\mathbb{X}' = \mathbb{X}'_- \cup \mathbb{X}'_+$, where $\mathbb{X}'_- = (-\infty, \underline{x})$ and $\mathbb{X}'_+ = (\bar{x}, \infty)$. We will prove the following lemma:

Lemma B.1 *Let \tilde{g} be the polynomial given in relation (18) of the main text, then for all $x \in \mathbb{X}'$, it is that $\liminf_{n \rightarrow \infty} \tilde{g}^{(n)}(x) = -\infty$ and $\limsup_{n \rightarrow \infty} \tilde{g}^{(n)}(x) = \infty$.*

Proof. It is not difficult to verify geometrically the following facts:

1. $\tilde{g}(\underline{x}) = \bar{x}$, $\tilde{g}(\bar{x}) = \underline{x}$.
2. $\underline{x} \leq x \leq \bar{x} \Leftrightarrow \underline{x} \leq \tilde{g}(x) \leq \bar{x}$.
3. $\tilde{g}(x) > x$, $\tilde{g}^{(2)}(x) < x$, $\forall x \in \mathbb{X}'_-$.
4. $\tilde{g}(x) < x$, $\tilde{g}^{(2)}(x) > x$, $\forall x \in \mathbb{X}'_+$.
5. The restrictions of \tilde{g} and $\tilde{g}^{(2)}$ to \mathbb{X}' , are decreasing and increasing functions respectively.

Then for all $x \in \mathbb{X}'_-$ we have the set of inequalities

$$\tilde{g}^{(2n+1)}(x) < \tilde{g}^{(2n-1)}(x) < \dots < \tilde{g}(x) < \underline{x}.$$

Suppose that $\lim_{n \rightarrow \infty} \tilde{g}^{(2n+1)}(x) = x^*$ then $\lim_{n \rightarrow \infty} \tilde{g}^{(2n+3)}(x) = \tilde{g}^{(2)}(x^*) = x^*$, meaning that $x^* \in \mathcal{R}^{(2)}$ which is a contradiction. Therefore $\lim_{n \rightarrow \infty} \tilde{g}^{(2n+1)}(x) = -\infty$, for all $x \in \mathbb{X}'_-$. Similarly for all $x \in \mathbb{X}'_+$ we have the set of inequalities

$$\tilde{g}^{(2n)}(x) > \tilde{g}^{(2n-2)}(x) > \dots > \tilde{g}^{(2)}(x) > \bar{x},$$

from which $\lim_{n \rightarrow \infty} \tilde{g}^{(2n)}(x) = \infty$, for all $x \in \mathbb{X}'_+$. □

Appendix C: Identification and prediction under noisy logistic observations

We have generated $n = 200$ observations from the random logistic map via

$$x_i = 1 - \vartheta x_{i-1}^2 + z_i, \quad 1 \leq i \leq 200,$$

for the initial condition $x_0 = 1$, and the control parameter $\vartheta = \vartheta^* = 1.71$. The random dynamical error z_i has been sampled independently from the noise process

$$f_{2,4} = \frac{9}{10}\mathcal{N}(0, \sigma^2) + \frac{1}{10}\mathcal{N}(0, (200\sigma)^2), \quad \sigma = 10^{-3}.$$

The time series dataset, has been generated in R under the random number generator seed $RNG_{f_{2,4}} = \{8\}$. The $f_{2,4}$ error process (see equation 20 in the main manuscript) produces the heaviest tail behavior as it exhibits the smaller TF measure (see the inequalities after equation 20 in the main manuscript). To test the ability of the parametric model (Param.) on the identification of the correct underlying model, we have modeled the associated deterministic part with a polynomial of degree $m = 5$ (there are six θ -coefficients $\{\theta_0, \dots, \theta_5\}$). We ran the parametric and GSBP samplers under noninformative prior specifications for simultaneous reconstruction and prediction for 5×10^5 after a burnin of 10^4 . The results are summarized in tables I and II. In Table 5, we provide the percentage absolute relative errors (PARE's) for the estimation of the control parameters and in Table 6 we present the PARE's based on the maximum a-posteriori (MAP) estimators, for the prediction of the first 5 future unobserved observations, for $T = 20$. In the last column of Table 6 we give the average PARE's obtained from the two methods.

Noise	Model	θ_0	θ_1	θ_2	θ_3	θ_4	θ_5	x_0
f_{24}	Param.	1.15	9.73	2.47	41.49	2.11	35.52	0.38
	GSBR	0.04	0.14	0.18	0.64	0.32	0.57	0.12

Table 5: Control parameter and x_0 PARE's based on the noisy logistic data set for $T = 20$.

Noise	Estim.	x_{201}	x_{202}	x_{203}	x_{204}	x_{205}	Average error
f_{24}	Param	13.52	5.10	28.67	123.14	137.67	61.62
	GSBR	0.89	0.39	1.54	4.01	2.80	1.93

Table 6: The first 5 out-of-sample PARE's based on the noisy logistic data set for $T = 20$.

Hence, it is clear that under a nongaussian noise process, the parametric Gibbs sampler cannot identify properly the true underlying model (in fact the parametric sampler predicts a quintic deterministic part). On the other hand, the GSBP sampler provides us with very accurate results; for example the average GSBP PARE for the θ -coefficients is 0.32 which is very small compared to the average parametric PARE which is 15.41.

Appendix D: Dynamical behavior of cubic map

While quadratic polynomial maps, can exhibit for each parameter value at most one stable attractor, multistability and coexistence of more than one strange attractors can be achieved under higher degree polynomial maps [20]. In this work, we illustrate the performance of the proposed model on a cubic map with complicated dynamical behavior. In particular, we perurbed with dynamical noise the random map with deterministic part

$$g(\vartheta, x) = 0.05 + \vartheta x - 0.99x^3 \quad (31)$$

fixing its controlling parameter at $\vartheta = \vartheta^* = 2.55$. Generally, when $\vartheta \in \Theta_{\text{bi}} = [\underline{\vartheta}_{\text{bi}}, \bar{\vartheta}_{\text{bi}}]$ with $\underline{\vartheta}_{\text{bi}} = 1.27$ and $\bar{\vartheta}_{\text{bi}} = 2.54$ the map becomes bistable. This means that in the phase space of the cubic map we can identify for $\vartheta \in \Theta_{\text{bi}}$, two mutually exclusive period-doubling cascades, together with two mutually exclusive basins of attractions. The dynamical behavior of the cubic map in (31) can be depicted in the bifurcation diagram shown in Figure 7. The coexisting attracting sets are plotted in blue and green.

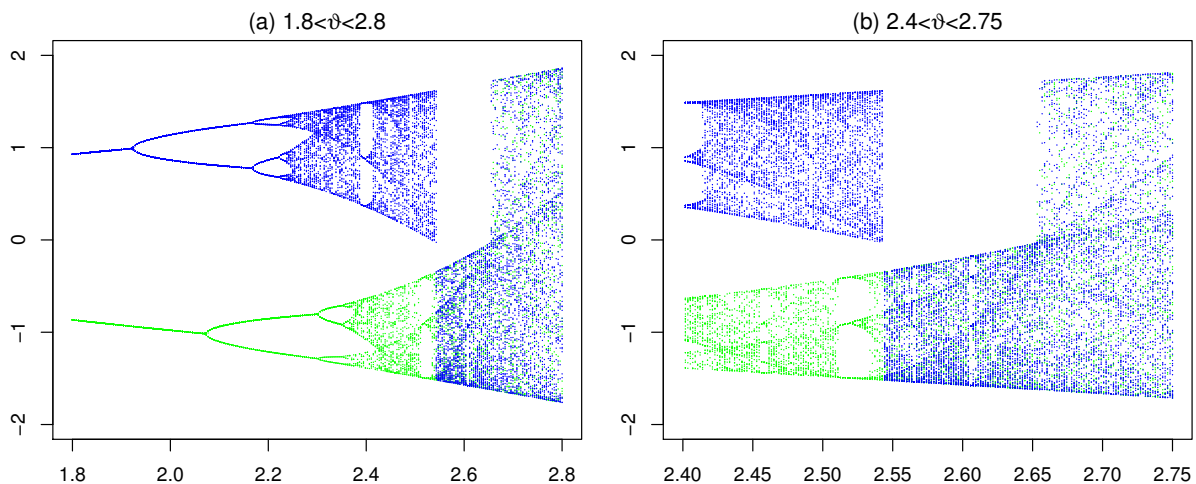


Figure 7: Bifurcation diagram of $g(\vartheta, x) = 0.05 + \vartheta x - 0.99x^3$.

We believe that the most intricate cases in terms of system identification and prediction are emanating from the dynamically perturbed time series when $\vartheta \in [2.54, 2.65]$. This is the case for $\vartheta = 2.55$, the value of the control parameter we have used in our numerical experiments. For this specific value of ϑ we have the coexistence of a repelling strange set $\mathcal{O}_{\text{unst},\infty}^+$ and an attracting strange set $\mathcal{O}_{\text{st},\infty}^-$. Letting $g(\vartheta, \cdot) \equiv g(\cdot)$, one has that

$$\mathcal{O}_{\text{unst},\infty}^+ \subset \bigcup_{r \geq 1} g^{(-r)}(\mathcal{O}_{\text{st},\infty}^-).$$

and all orbits will be eventually attracted by the “lower” part $\mathcal{O}_{\text{st},\infty}^-$. Nevertheless when the $f_{2,4}$ dynamical noise is present, the random orbits (in red) are able to visit the vicinity of the repelling set $\mathcal{O}_{\text{unst},\infty}^+$, ad infinitum, as we show in Figure 8.

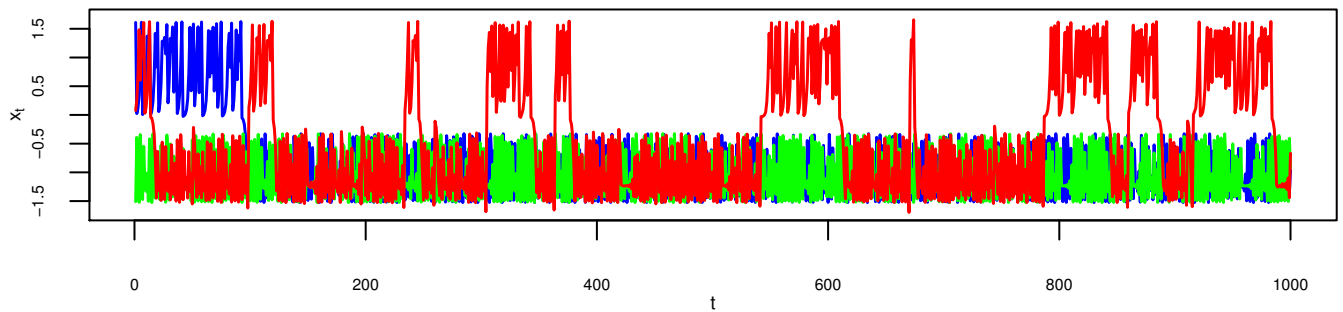


Figure 8: Orbits of $g(\vartheta, x) = 0.05 + \vartheta x - 0.99x^3$, with $\vartheta = 2.55$. Blue and green show deterministic orbits, red shows noisy orbit.

References

- [1] Henry Abarbanel. *Analysis of observed chaotic data*. Springer Science & Business Media, 2012.
- [2] Ludwig Arnold. *Random dynamical systems*. Springer Monographs in Mathematics. Springer-Verlag, Berlin, 1998.
- [3] L Mark Berliner. Statistics, probability and chaos. *Statistical Science*, pages 69–90, 1992.
- [4] Sangit Chatterjee and Mustafa R Yilmaz. Chaos, fractals and statistics. *Statistical Science*, pages 49–68, 1992.
- [5] ME Davies. Nonlinear noise reduction through Monte Carlo sampling. *Chaos: An Interdisciplinary Journal of Nonlinear Science*, 8(4):775–781, 1998.
- [6] Thomas S Ferguson. A Bayesian analysis of some nonparametric problems. *The annals of statistics*, pages 209–230, 1973.
- [7] R. Fuentes-García, R. H. Mena, and S. G. Walker. A new Bayesian nonparametric mixture model. *Comm. Statist. Simulation Comput.*, 39(4):669–682, 2010.
- [8] Georg M Goerg. Forecastable component analysis. In *ICML (2)*, pages 64–72, 2013.
- [9] Georg M. Goerg. *ForeCA: An R package for Forecastable Component Analysis*, 2016. R package version 0.2.4.
- [10] Stephen M Hammel. A noise reduction method for chaotic systems. *Physics letters A*, 148(8-9):421–428, 1990.
- [11] Spyridon J Hatjispyros, Theodoros Nicolieris, and Stephen G Walker. A Bayesian nonparametric study of a dynamic nonlinear model. *Computational Statistics & Data Analysis*, 53(12):3948–3956, 2009.

- [12] JPM Heald and J Stark. Estimation of noise levels for models of chaotic dynamical systems. *Physical review letters*, 84(11):2366, 2000.
- [13] Borchers H.W. *pracma: Practical Numerical Math Functions*,, 2015. R package version 1.8.3.
- [14] Lars Jaeger and Holger Kantz. Homoclinic tangencies and non-normal jacobian effects of noise in nonhyperbolic chaotic systems. *Physica D: Nonlinear Phenomena*, 105(1):79–96, 1997.
- [15] Nouha Jaoua, Emmanuel Duflos, Philippe Vanheeghe, and François Septier. Bayesian nonparametric state and impulsive measurement noise density estimation in nonlinear dynamic systems. In *2013 IEEE International Conference on Acoustics, Speech and Signal Processing*, pages 5755–5759. IEEE, 2013.
- [16] Kiyoshi Kanazawa, Tomohiko G Sano, Takahiro Sagawa, and Hisao Hayakawa. Asymptotic derivation of langevin-like equation with non-gaussian noise and its analytical solution. *Journal of Statistical Physics*, 160(5):1294–1335, 2015.
- [17] Kiyoshi Kanazawa, Tomohiko G Sano, Takahiro Sagawa, and Hisao Hayakawa. Minimal model of stochastic athermal systems: Origin of non-gaussian noise. *Physical review letters*, 114(9):090601, 2015.
- [18] Holger Kantz and Thomas Schreiber. *Nonlinear time series analysis*, volume 7. Cambridge university press, 2004.
- [19] Eric J Kostelich and James A Yorke. Noise reduction in dynamical systems. *Physical Review A*, 38(3):1649, 1988.
- [20] Suso Kraut, Ulrike Feudel, and Celso Grebogi. Preference of attractors in noisy multistable systems. *Physical Review E*, 59(5):5253, 1999.
- [21] Krzysztof Łatuszyński, Gareth O Roberts, Jeffrey S Rosenthal, et al. Adaptive gibbs samplers and related mcmc methods. *The Annals of Applied Probability*, 23(1):66–98, 2013.
- [22] Albert Y Lo et al. On a class of Bayesian nonparametric estimates: I. density estimates. *The annals of statistics*, 12(1):351–357, 1984.
- [23] Dmitri G Luchinsky, Vadim N Smelyanskiy, Andrea Duggento, and Peter VE McClintock. Inferential framework for nonstationary dynamics. i. theory. *Physical Review E*, 77(6):061105, 2008.

- [24] Takashi Matsumoto, Yoshinori Nakajima, Motoki Saito, Junjiro Sugi, and Hiroaki Hamagishi. Reconstructions and predictions of nonlinear dynamical systems: A hierarchical Bayesian approach. *IEEE transactions on signal processing*, 49(9):2138–2155, 2001.
- [25] Patrick E McSharry and Leonard A Smith. Better nonlinear models from noisy data: Attractors with maximum likelihood. *Physical Review Letters*, 83(21):4285, 1999.
- [26] Ramsés H Mena, Matteo Ruggiero, and Stephen G Walker. Geometric stick-breaking processes for continuous-time bayesian nonparametric modeling. *Journal of Statistical Planning and Inference*, 141(9):3217–3230, 2011.
- [27] Renate Meyer and Nelson Christensen. Bayesian reconstruction of chaotic dynamical systems. *Physical Review E*, 62(3):3535, 2000.
- [28] Renate Meyer and Nelson Christensen. Fast Bayesian reconstruction of chaotic dynamical systems via extended kalman filtering. *Physical Review E*, 65(1):016206, 2001.
- [29] David Middleton. Statistical-physical models of electromagnetic interference. *IEEE Transactions on Electromagnetic Compatibility*, (3):106–127, 1977.
- [30] YI Molkov, EM Loskutov, DN Mukhin, and AM Feigin. Random dynamical models from time series. *Physical Review E*, 85(3):036216, 2012.
- [31] Mark R Muldoon, David S Broomhead, Jeremy P Huke, and Rainer Hegger. Delay embedding in the presence of dynamical noise. *Dynamics and Stability of Systems*, 13(2):175–186, 1998.
- [32] Yohei Nakada, Takashi Matsumoto, Takayuki Kurihara, and Kuniaki Yosui. Bayesian reconstructions and predictions of nonlinear dynamical systems via the hybrid Monte Carlo scheme. *Signal processing*, 85(1):129–145, 2005.
- [33] Radford M Neal et al. Mcmc using hamiltonian dynamics. *Handbook of Markov Chain Monte Carlo*, 2:113–162, 2011.
- [34] Takuya Nishimoto, Yoko Uwate, Yasuteru Hosokawa, Yoshifumi Nishio, Daniele Fournier-Prunaret, and Abdel-Kaddous Taha. Bifurcation and basin in two coupled cubic maps.
- [35] Edward Ott. *Chaos in dynamical systems*. Cambridge university press, 2002.
- [36] Steven M Pincus. Approximate entropy as a measure of system complexity. *Proceedings of the National Academy of Sciences*, 88(6):2297–2301, 1991.
- [37] Christian Robert. *The Bayesian choice: from decision-theoretic foundations to computational implementation*. Springer Science & Business Media, 2007.

- [38] David Ruelle and Floris Takens. On the nature of turbulence. *Communications in mathematical physics*, 20(3):167–192, 1971.
- [39] Jayaram Sethuraman. A constructive definition of Dirichlet priors. *Statistica sinica*, pages 639–650, 1994.
- [40] Jayaram Sethuraman and Ram C Tiwari. Convergence of Dirichlet measures and the interpretation of their parameter. Technical report, DTIC Document, 1981.
- [41] M Shinde and S Gupta. Signal detection in the presence of atmospheric noise in tropics. *IEEE Transactions on Communications*, 22(8):1055–1063, 1974.
- [42] M Siefert, M Kern, R Friedrich, and J Peinke. How to differentiate quantitatively between nonlinear dynamics, dynamical noise and measurement noise. In *Experimental Chaos: 8th Experimental Chaos Conference*, volume 742, pages 337–344. AIP Publishing, 2004.
- [43] M Siefert and J Peinke. Reconstruction of the deterministic dynamics of stochastic systems. *International Journal of Bifurcation and Chaos*, 14(06):2005–2010, 2004.
- [44] Silke Siegert, R Friedrich, and J Peinke. Analysis of data sets of stochastic systems. *arXiv preprint cond-mat/9803250*, 1998.
- [45] VN Smelyanskiy, Dmitry G Luchinsky, DA Timucin, and A Bandrivskyy. Reconstruction of stochastic nonlinear dynamical models from trajectory measurements. *Physical Review E*, 72(2):026202, 2005.
- [46] LA Smith and A Mees. Nonlinear dynamics and statistics. *Disentangling Uncertainty and Error: On the Predictability of Nonlinear Systems*, Birkhäuser, Boston, 2000.
- [47] Marek Strumik and Wieslaw M Macek. Influence of dynamical noise on time series generated by nonlinear maps. *Physica D: Nonlinear Phenomena*, 237(5):613–618, 2008.
- [48] Stephen G Walker. Sampling the Dirichlet mixture model with slices. *Communications in Statistics–Simulation and Computation*®, 36(1):45–54, 2007.
- [49] Mike West. *Hyperparameter estimation in Dirichlet process mixture models*. Duke University ISDS Discussion Paper# 92-A03, 1992.